

The Basic Architecture of the System with the A-GNSS Receiver

Lucjan Setlak^{1*}, Rafał Kowalik^{1*}

¹Department of Avionics and Control Systems, Polish Air Force University, ul. Dywizjonu 303 nr 35, 08-521 Deblin

Abstract. The paper presents the results of obtained research defining the accuracy of determining the position of a specific object (aircraft, UAV), equipped with a mobile receiver operating the navigation system A-GNSS. The Assisted GNSS technology is designed to improve the performance of the GNSS receiver by reducing the time needed for the receiver to calculate its location. It also increases the sensitivity of the received signal by the receiver, as a result, the accuracy of the determined position of a specific object can be improved. Thanks to its application, the radio-navigation receiver becomes compatible with the requirements of current standards, and what is associated with it this kind of technology has become an important part of the cellular industry. The aim of the article is to examine the solution of A-GPS system and to demonstrate its effectiveness in the process of determining the position of the UAV object. The paper presents aspects of the functionality of the A-GPS system solution work, mathematical model of object position determination using A-GNSS system and discusses the technology that is used for the integration of navigation systems with cellular network. In the final part of the work, based on the analysis of the research literature, the presented mathematical model and simulations, conclusions were formulated, which are reflected in practical applications.

1 Introduction

Assisted global navigation satellite system A-GNSS (*Assisted Global Navigation Satellite System*) significantly improves the standard performance of satellite systems by providing information through an alternative communication channel, which is a cellular link, compared to a standard receiver that acquires information from the satellites themselves. It should be noted that the A-GNSS system receiver still performs measurements from satellites, but it can do it faster and with weaker received signals in analogy to the standard receiver.

Each satellite of the satellite navigation system GPS (*Global Positioning System*) sends a data stream through the pseudorandom PRN (*Pseudo Random Noise*) code, but when the signal moves over the obstacles, it becomes weaker and the data may not be detectable, but the code still exists. The assisted global positioning system A-GPS (*Assisted Global Positioning System*) provides the same or equivalent data via a cellular antenna network. The A-GPS receiver receives the same information that it could get from the satellite if the signal was not blocked [1], [2], [3].

This type of concept also allows the A-GPS system receiver to calculate the position faster, even if the previous satellite signal is not memorized, because the data can be acquired much faster from the local cellular antenna than from the satellite. Satellite data is collected and processed by the network of reference stations and the A-GNSS system location server. While the auxiliary

data are usually, but not necessarily, provided by a wireless network or a cellular data channel.

The approximate position of the A-GNSS system receiver is immediately sent after it has been processed by a cellular antenna, as illustrated in the data transfer diagram (Fig. 1).

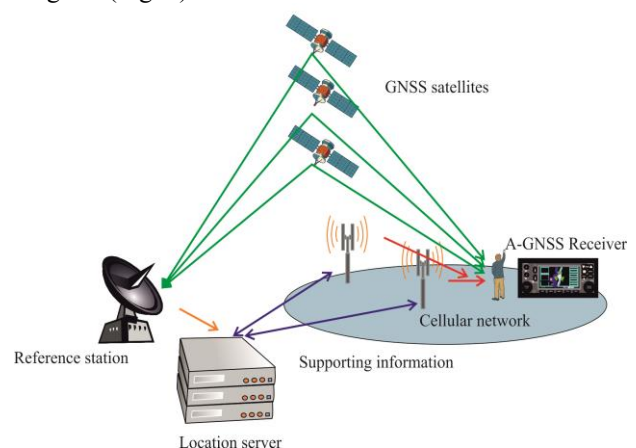


Fig. 1. A scheme of transmitting data to the A-GNSS system receiver.

The assisted A-GPS system functions by providing information that allows the GPS system receiver to determine what frequencies should be expected before sending them, and then acquire auxiliary data that provides satellite positioning for use in calculating the position of the receiver. With all this data, the only thing left to do at this time is to measure the range, which can be done in milliseconds [ms], not in minutes [min].

* Corresponding author: l.setlak@wsosp.pl, r.kowalik@wsosp.pl

In view of the above, the total time of receiving the first desired position is shortened from 1 [min] to 1 [s]. In addition, because the A-GPS system receiver was designed in the way to have information in advance what are the search frequencies, with the typical receiver architecture changing to allow longer waiting times that increase the amount of energy received at each particular frequency. As a result, the sensitivity of the A-GPS system receiver is increased, which allows it to obtain signals with much lower power [4], [5].

2 The operating principle of the standard GNSS system receiver

A navigation system receiver without information on priority frequencies will have to search their large ranges, consisting largely of the effects of satellite motion and the receiver oscillator shift and the small contribution of the speed of the receiver. The standard receiver has to search 8.4 [kHz] of unknown frequencies due to the *Doppler* effect and the movement of the satellites. Usually there is a small *Doppler* effect caused by the speed of the receiver, i.e. up to 1.5 [Hz] for every 1 [km/h] of speed. An additional 1.5 [kHz] of unknown frequency shift is created for every 1 ppm (*parts per million*) of an unknown offset of the receiver oscillator.

Thus, the total range of unknown frequency is in the range from 10 to 25 [kHz], and a typical receiver can search them in groups of approximately 500 [Hz] each, which means a search of the range of about 20-50 groups.

Therefore, the receiver without prior knowledge of the code delay will also have to search all possible intervals of its delay. For example, in the acquisition mode, the correlator is usually set to 0.5 code, which means 2 correlators for each PRN code, the total amount of code delay is 1023. The traditional GPS receiver will have 2 correlators per channel and so it is possible to search one code at a time. Therefore, with an integration time of 1 [ms], which corresponds to the duration of the PRN code, the A-GNSS system receiver could take 1 [s] to search for all 1023 possible delays.

In addition, it should be noted that the standard receiver without initial knowledge performs, so-called "cold start" and must search the two-dimensional space with frequency bands and code delay systems.

This type of search requires at least 20 [s] slightly more than 1 [s] to search for all 1023 possible code delays in each frequency range. In the case where a correlation peak is found for each satellite, the search is completed, but the receiver can not calculate the position until it decodes the weekday data and ephemeris data, and the received data is transmitted every 30 [s], so the expected decoding time is also 30 [s], while the total time of the first repair is approximately 1 [min], at least for this receiver [6], [7], [8].

If the signal is blocked or disappears, even for a few milliseconds, data errors may occur during this time, and the receiver will have to wait another 30 [s] for the data to be retransmitted. It should be added that a conventional receiver will take several minutes to get the

first correction when the signal is weak due to the environment, e.g. under trees or in a dense urban area.

Typically, the standard navigation system receiver has the following data, which may help to some extent with initial measurements, namely:

- the approximate position, compared to the last position stored in the memory,
- approximate time from real-time clock,
- approximate image of the reference frequency, since the offset will be determined at the last start of the receiver, and this value is usually stored in the memory.

The receiver that is run in this state performs the so-called "warm start". In this case, the number of frequency boxes can be significantly reduced. However, the navigation system receiver must still decode the time of the week and ephemeris to calculate the position, so the expected warm-up time to obtain a correction will still be greater than 30 [s].

If the above receiver has already decoded the ephemeris for all visible satellites and the calculated position, then it was turned off and turned on a few minutes later, then this kind of condition is referred to as "hot start". In this case, the initial knowledge of the receiver is very good, but analogically, as in the case of "warm start", the receiver has a reduced number of frequency boxes to search [9], [10].

On the other hand, if the clock was good enough in real time, then the time could be known better than a millisecond, and the receiver can also reduce the search space of the code delay, and the acquisition time can be reduced to less than 1 [s]. Due to the fact that the time is already known exactly, the time of the week does not have to be decoded, so the ephemeris are already known.

In this case, the correction time may be less than 1 [s] and this is the type of data acquisition characteristic of the A-GNSS system receiver.

3 Assistance obtained by the A-GNSS system receiver along with its comparison to conventional means

The first and most obvious function of the A-GNSS navigation system is to deliver ephemeris data to the receiver so that it does not have to decode their transmittance. As mentioned earlier (chapter 2), it is also used to reduce the range of frequency searches and code delays. In turn, to reduce the frequency search space, at least the approximate position of the satellite is necessary. The expected frequencies after passing the *Doppler* effect can then be calculated. Therefore, to reduce the search area of the code delay, it is necessary to specify the exact time where the code delay can be up to 1 [ms], so the advance time must be less than 1 [ms].

For example, if in 1 [ms] the GPS system signal travels a distance of 300 [km] at the speed of light, then the location must be known for more than 150 [km] to be able to use the exact time as the basic datum. Typically, in the A-GPS system, the position is known a few kilometers from the location of cellular antennas, however, the exact time is not known as the time

specified above. If the obtained time, however, is shorter than 1 [ms], it is referred to as so-called good time help. In aviation, there are two main types of approach to landing with a GPS system receiver, known as *MS-assisted* and *MS-based*, where "MS" means a mobile station, i.e. a GPS system receiver [11], [12],[13]. In the assisted mode of the mobile station GPS system (*Mobile Station Assisted GPS*), the position is calculated on the server, and the task of the GPS system receiver is only to acquire signals and send measurements to the server. In the case of a "hot start", the standard receiver would have knowledge of the last position, time and shift of the receiver oscillator. In the case of the A-GPS system, the receiver may have not been turned on recently, but will receive enough information in the auxiliary data to have the same accuracy as for the "hot start" of the conventional receiver.

The relative *Doppler* frequency of the satellite of the GPS system on the L1 band, when viewed from the GPS system receiver on Earth, oscillates in the range, from -4.2 to 4.2 [kHz], as the one sent and received, the rate of change of this *Doppler* frequency is up to 0.8 [Hz/s]. Therefore, for every error during 1 [s], the expected *Doppler* frequency may be erroneous up to a value of 0.8 [Hz]. It should be noted that *Doppler* coefficients usually have negative values, because if the satellite sends a signal to the recipient, its *Doppler* value is positive, while when it reaches its zenith, this frequency reaches the value of 0, and if the signal is away from the recipient, gains negative values. Thus, the total trend of *Doppler* effect for the satellite is positive to zero, and the average speed of the effect is negative.

The following figure (Fig. 2) shows the observed *Doppler* velocities for all satellites within 24 hours, observed from various locations on the surface of the Earth.

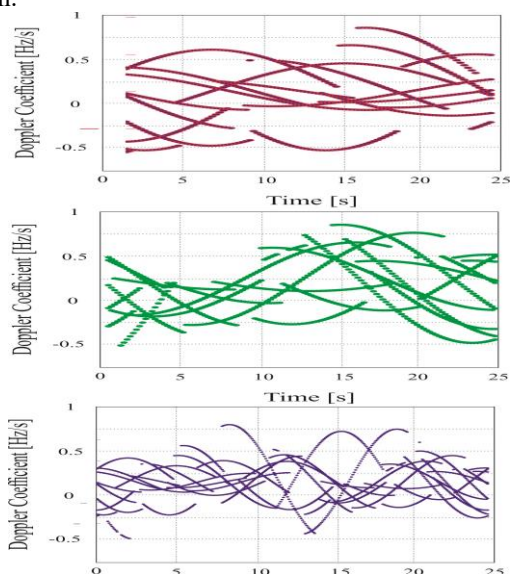


Fig. 2. Doppler coefficient for different latitudes.

When analyzing this figure, one can observe how the *Doppler* rates change with the change in latitude. For example, at the North Pole, the rotation of the Earth has no effect on the observed satellites, so the *Doppler* indicators behave in a simple and consistent way for all satellites [14], [15].

In turn, along with approaching the equator, the observed *Doppler* velocities are more complicated, because the navigation system receiver rotates under the orbit of the satellite, the same phenomenon exists for the southern hemisphere. The main point in the picture is that the maximum *Doppler* speed is 0.8 [Hz/s].

3.1. Error analysis in the auxiliary frequency range: reference frequency and speed

The reference frequency error has a 1:1 effect on the expected values of the *Doppler* coefficient. In the case of applications for mobile phones, this value is calculated using the frequency from a telephone voltage controlled oscillator coded to the signal from the cellular network antenna.

The cellular antenna frequency is known at ± 50 ppb (*parts per billion*) on the cell tower and ± 100 ppb on the mobile phone, so it is necessary to take into account the error of ± 100 ppb for the expected *Doppler* effect. If the receiver is in motion, the Doppler frequency may increase up to 1.46 [Hz] per 1 [km/h] of speed.

There is also a speed effect on the supported reference frequency, from the frequency obtained from the cell tower. By moving the receiver towards the cellular antenna, the observed cellular frequency will increase by about 1 ppb for every 1 [km/h] of speed, as a consequence of which this phenomenon will affect the reference frequency of the GPS system in the same proportion. However, if the receiver moves away from the antenna, the effect is the same, but its value is negative.

It should be noted that the *Doppler* effect on velocity is often more visible on the reference frequency than on satellite frequencies because, receivers necessarily have to be directly in the vicinity of the antennas and interact with them, but rarely move directly towards the satellite.

3.1.1 Analysis of auxiliary frequency errors related to position

The error of the auxiliary frequency having an influence on the position indication is connected with the error in the observed GPS system signal, because the received *Doppler* frequency is a function of what the receiver obtains from the satellite. The *Doppler* effect factor from the satellite is equal to the product of velocity vectors with the line of observation from the user to the satellite, as shown in the next figure (Fig. 3).

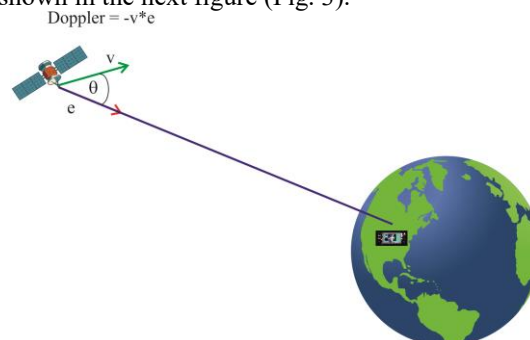


Fig. 3. Vectors of the Doppler coefficient for the satellite.

The position error causes a line of sight error. The error of *Doppler* satellites is approximately equal to the product of velocity vectors and the difference between the two lines of real and expected observation, i.e.:

$$\delta = v * (e_{real} - e_{expected}). \quad (1)$$

The value resulting from the presented formula (1) is approximate, because the angle θ_{real} between e_{real} and the speed of the satellite is slightly different from the angle $\theta_{expected}$. The reason for this approximation is that it allows you to analyze the *Doppler* error for satellites in terms of the size of the position error that causes it. In terms of the position error vector, a below formula (2)

$$\delta = (e_{real} - e_{expected}) \text{ £ } \delta x / coverage. \quad (2)$$

is obtained.

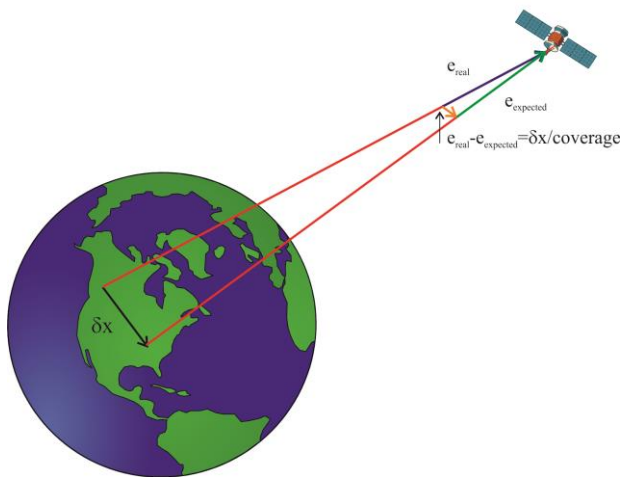


Fig. 4. The position of the largest Doppler error.

This can be seen on the basis of the analysis of the figure above (Fig. 4). The worst case error ($=\delta x / coverage$) occurs when the position error is such that it forms the basis of the isosceles triangle, as shown in the figure. Because the satellites are far away, the worst case position is achieved when the direction is almost perpendicular to the line of sight.

This type of situation will not occur when the position error is in the same direction (or opposite) as the line of sight, because in these cases the line of sight does not change at all, so the calculated *Doppler* factor will be correct, where the position error shown in the figure is large, for visual clarity [16, [17], [18].

In practical applications, a typical position error for the A-GNSS system receiver covers several kilometers, while the *Doppler* error for a satellite is determined by the following relationships (3) - (5):

$$\delta \text{ £ } v \delta x / coverage, \quad (3)$$

$$\text{£ Satellite speed } \frac{1}{2} \delta x \frac{1}{2} / coverage, \quad (4)$$

$$\text{£ } 3,8 * 10^3 \frac{1}{2} \delta x \frac{1}{2} / (2 * 10^7) [m/s] = 0,19 * 10^{-3} \frac{1}{2} \delta x \frac{1}{2} [m/s]. \quad (5)$$

Thus, for a position estimation error of 1 [km], a maximum satellite *Doppler* error of around $0.19 [m/s] =$

$1 [Hz]$ (in the L1 band) was obtained.

Generating for each 1 [km] position error, the induced satellite *Doppler* error is a maximum of 1 [Hz].

Table 1. Differences in velocity and Doppler error calculated from ephemeris and information on the status of constellation of satellites called almanac [17].

	50th percentile	99th percentile	Largest error
$ v_{ephemeris} - v_{almanac} $	0.49 [m/s]	11.77 [m/s]	31.12 [m/s]
$L_1 * v_e - v_a / c$	2.6 [Hz]	618 [Hz]	163.4 [Hz]

3.1.2 Analysis of auxiliary frequency errors in terms of almanac and ephemeris influence

In order to calculate the expected satellite traffic, the navigation system receiver can use either almanac, i.e. information on the time and status of the entire satellite constellation or ephemeris, which can be provided in the help of the mobile station receiver system MS (*Mobile Station*). The velocity accuracy of ephemeris is essentially ideal, i.e. 1 [mm/s], which corresponds to *Doppler* accuracy 1 [mHz].

The above table (Table 1) shows the distribution of the speed difference of the satellite calculated from the almanac and the speed of the satellite calculated from ephemeris. This table also presents the size difference of velocity vectors $|v_e - v_a|$, where v_a is the satellite velocity vector calculated using the almanac, and v_e is the vector of the satellite velocity calculated using ephemeris.

The effect of these speed errors on the calculated satellite *Doppler* error depends on the angle between the error vector $(v_e - v_a)$ and the user's line of vision, denoted as θ . The calculated satellite *Doppler* error would then be $L_1 |v_e - v_a| \cos(\theta) / c$, where L_1 is the frequency of the GPS system $L_1(1575.42 [MHz])$, while c is the speed of light. The last line of the table shows *Doppler* errors for the worst position $\cos(\theta) = 1$.

It should also be noted that the biggest error is many times greater than the median error and even the 99th percentile. Thus, although the worst case of error is large, constellation status information can still be used for frequency support of A-GNSS system receivers.

For example, in the context of the above reasoning, the situation is as follows that using frequency almanac data, frequency search is designed to cover $\pm 60 [Hz]$. Then the frequency error from the almanac is marked for about 1 [%] of time. However, this error is a function of the satellite view line, so it does not apply to connections between them. This means that 1 [%] frequency error covers individual satellites, the consequence of this error being the possibility of not intercepting the satellite.

The probability of two satellites simultaneously means the frequency error from the almanac on the level of about 1 [%] to the square (in the example shown), that is 10^{-4} , etc. The probability of more satellites with simultaneous frequency error from the almanac becomes exponentially smaller [19], [20].

Therefore, the almanac can be used to calculate the

frequency aid with a high probability that the correct frequency will be obtained at least for the majority of satellites in the view.

3.2. A-GNSS system receiver assistance for code delay

Time is helpful in determining the frequency, because a time, at least approximate, is required to calculate the expected satellite speed, and consequently to determine the expected *Doppler* error. However, it should be noted that time also helps to estimate code delays. The code delay is a function of the position of the navigation system receiver and the time of the receiver clock that generates the local correlation delay. The full range of possible delay of GPS C/A (*Coarse Acquisition*) codes is 1 [ms], and then the code repeats itself.

Satellites of GPS navigation systems send 2 types of signals in the form of codes, namely: C/A code ($L1 = 1575.42$ [MHz]) for SPS (*Standard Positioning Service*) users and a code for PPS (*Precise Positioning Service*) users, i.e. for $L2$ frequency = 1227.6 [MHz] (military applications). In the case of normal reception, the above codes in the context of the analogy with the noise signal, resemble illusory noise, hence they are called pseudorandom PRN signals, whereby the C/A code is a digital signal which is transmitted at a transmission rate of 1.023 [MHz]. The analogy of this signal with the noise signal was created in the context of its long repetition period, i.e. every 1023 bits. In addition, this type of sequence is different for each satellite and is defined in the form of a PRN code.

Based on the above, the receivers of navigation systems have the ability to distinguish between signals originating from individual sources, where the P (*Precise*) code is falsely similar, but has a more complex structure compared to the C/A code.

In a situation where the time of the receiver of the navigation system is not known more than 1 [ms], the estimated delay of the code can not be given. In this case, the A-GPS system receiver will have to search all possible code delays in each frequency range in the way it is done based on the classical navigation receiver.

For example, if the receiver's time is accurate to 1 [ms], then the accuracy of the A-GNSS system in determining the position becomes important for the purpose of searching for the code delay. However, if the accuracy of the receiver's position is lower than 150 [km], the expected code delay will be ambiguous up to ± 150 [km], i.e. 300 [km], or 1 [ms] code delay, as in 1 [ms] at the speed of light a section of about 300 [km] is covered.

It should be noted that the effect of position error is a bit more complicated due to the direction of the error and the height of the satellite. At the outset, it's enough to assume that the external limits of time accuracy and position accuracy are 1 [ms] and 150 [km], respectively, to help search for code delays. There are several cellular networks, however, not every one has microsecond timing accuracy, sufficient to provide assistance in finding code delays [21], [22], [23].

The only CDMA (*Code-division Multiple Access*) network is capable of this, which means a multi-access network with code division. There are network synchronization initiatives to provide a greater range of time. One of the basic ideas is that each A-GPS system receiver, satellite tracking system, can be used to synchronize the network for the benefit of other A-GPS system receivers in the same network.

3.3. Time data transmitted by the cellular A-GNSS system receiver to the general network

Most A-GNSS system receivers have the ability, after intercepting the satellite, to decode the satellite data. Because such A-GPS system receivers are connected to a network, e.g. a cellular one, this makes it possible to use the A-GPS mobile system receiver as a source of auxiliary data in the network in particular, real time synchronization and orbital data. However, the most widespread cellular networks in the world in the GSM standard (*Global System for Mobile Communications*) and the 3G UMTS standard (*Universal Mobile Telecommunications System 3rd Generation*), do not have synchronized antennas with precise accuracy.

So, the only thing that can be gained is if A-GPS systems receivers using these networks will be able to synchronize back time to the part of the network to which they are connected. In the event that any GPS system receiver decoded the satellite signal, this information is provided within 12 [ms].

However, when the same receiver calculates its position, it will know the flight time within nanoseconds, and thus will know the time of day with an accuracy of 1 [ms]. The same receiver of the navigation system can compare the obtained time with the time provided by the network and can thus calculate the time offset of the base station to which it is connected [24], [25].

If this information is then shared with other receivers of the A-GPS system connected to the same base station, it provides them with precise time assistance. This kind of idea has been included and implemented in the A-GPS system standards.

4 Calculation of positions from Doppler data

In the case where the device uses the ephemeris extensions, it is able to calculate the position without first decoding the data obtained from each of the satellites. The advantage of this is, above all, faster time of obtaining corrections and repairing weak signals. With ephemeris extensions, but without exact position, wait until the signal is decoded on several satellites, and then the position will be calculated using the resulting full pseudo-distances.

An additional way is to generate an initial position using *Doppler* measurements from satellites, where the *Doppler* frequency is a function of the velocity of the satellite. When the satellite is moving exactly towards the navigation system receiver, the positive *Doppler*

frequency corresponding to the satellite velocity $|v|$ is measured [26], [27], [28].

Then it is known that the position line of the navigation system receiver is indicated by the satellite speed vector. If a positive *Doppler* frequency of smaller size $|v| \cos(\alpha)$ is measured, then it is calculated on the cone shown in the figure below (Fig. 5).

However, if the zero *Doppler* frequency is measured, the satellite moves perpendicular to the direction in the view of the recipient. When negative frequencies are taken into account, the satellite moves away from the receiver and again the surface of the position is a cone.

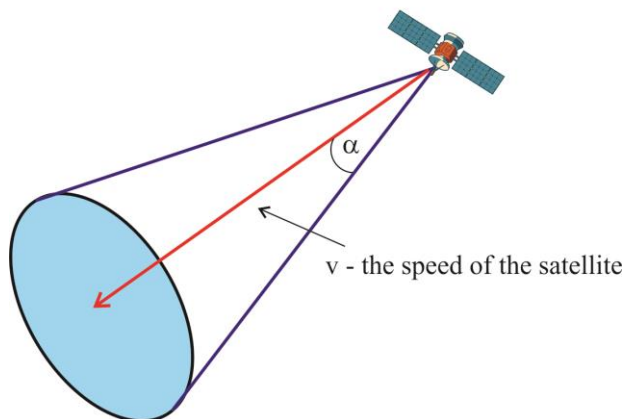


Fig. 5. A cone showing the position surface derived from the *Doppler* frequency measurement from a known point and the known satellite speed.

4.1. Analysis of the mathematical navigation system

By deriving navigational equations with partial derivatives, you can implement them in software calculating the position from the *Doppler* data itself or in combination with pseudo-distance data [29], [30].

Initially, the linear navigation equation should be presented in relation to the updated pseudo-distance (6):

$$\delta z = H\delta x + \varepsilon, \quad (6)$$

where:

δz - is the vector of the resonance of the measurement resonance of the pseudo-distance $\delta z = z - z^{\wedge}$,

z - is a vector of the measured pseudo-distance,

z^{\wedge} - is a vector of the predicted pseudo-distance,

H - is an observation matrix,

$\delta x = \begin{bmatrix} \delta x \\ \delta y \\ \delta z \\ \delta b \end{bmatrix}$ - is a vector of updating the status of positions

x, y, z and b ,

ε - is a vector of measurement errors and linearization.

Both sides of the equation were divided by the time t and obtained the following (7):

$$\frac{\delta z}{t} = \frac{(z - z^{\wedge})}{t} = \frac{H\delta x}{t} + \varepsilon', \quad (7)$$

$$\frac{z}{t} - \frac{z^{\wedge}}{t} = H \frac{(\delta x)}{t} + \frac{H}{t} \delta x + \varepsilon'.$$

The left side is the result of accurate measurements of the original *Doppler* effect, otherwise $\delta y = y - \hat{y}$, where:

$y := \frac{z}{t}$ - is a vector of the measured *Doppler* effect,

$\hat{y} := \frac{\hat{z}}{t}$ - is the vector of the expected *Doppler* effect.

The conditions on the right can be evaluated as follows. The first part is recognizable from the classic linear equation for the receiver's speed, which can be written in the following form (8):

$$H \frac{(\delta x)}{t} = \frac{H \begin{bmatrix} \delta x \\ \delta y \\ \delta z \\ \delta b \end{bmatrix}}{t} = H \begin{bmatrix} \delta x \\ \delta y \\ \delta z \\ \delta b \end{bmatrix}, \quad (8)$$

where:

$\delta x, \delta y, \delta z$ - are updates of the initial velocity states of the receiver of the navigation system, and δb - is the update of the original state of the frequency shift.

The second part is the part that shows the connection between the given position and the *Doppler* effect measurements (9):

$$\frac{H}{t} \delta x = \frac{\begin{bmatrix} -e^{(1)} & \dots & 1 \\ \vdots & \dots & \vdots \\ -e^{(K)} & \dots & 1 \end{bmatrix} \begin{bmatrix} \delta x \\ \delta y \\ \delta z \\ \delta b \end{bmatrix}}{t}$$

$$= \begin{bmatrix} -e^{(1)} & / & t & 0 \\ \vdots & \dots & \vdots & \\ -e^{(K)} & / & t & 0 \end{bmatrix} \begin{bmatrix} \delta x \\ \delta y \\ \delta z \\ \delta b \end{bmatrix} \quad (9)$$

$$= \begin{bmatrix} -e^{(1)} & / & t \\ \vdots & \dots & \vdots \\ -e^{(K)} & / & t \end{bmatrix} \begin{bmatrix} \delta x \\ \delta y \\ \delta z \\ \delta b \end{bmatrix},$$

To evaluate the above equation (9) it is necessary to find the expression for 3-vector $[e^{(k)}/t]$ (10).

$$\frac{\partial e^{(k)}}{\partial t} = \frac{\partial}{\partial t} \left(\frac{x^{(k)} - x_{xyz0}}{|x^{(k)} - x_{xyz0}|} \right), \quad (10)$$

where:

$x^{(k)}$ - is the position of the satellite k ,

x_{xyz0} - is the original position of the receiver.

For the sake of simplifying the calculation of the above equation (10), the superscript k will be replaced with r , corresponding to the range of the satellite:

$r = |x - x_{xyz0}|$, as shown in the following equation (11).

$$\frac{\partial e}{\partial t} = \frac{\partial}{\partial t} \left(\frac{x - x_{xyz0}}{r} \right)$$

$$= \left(\frac{\partial(x - x_{xyz0})}{\partial t} \cdot r - (x - x_{xyz0}) \cdot \frac{\partial r}{\partial t} \right) \frac{1}{r^2} \quad (11)$$

$$\begin{aligned}
 &= \left(\frac{\partial(x)}{\partial t} \cdot r - (x - x_{xyz0}) \cdot (e \cdot v) \right) \frac{1}{r^2} \\
 &= \left(\frac{\partial(x)}{\partial t} \cdot r - r \cdot e \cdot (e \cdot v) \right) \frac{1}{r^2} \\
 &= \left(\frac{\partial(x)}{\partial t} - e \cdot (e \cdot v) \right) \frac{1}{r}.
 \end{aligned}$$

As can be seen, the above formula (11) consists of a difference in the relative speed of the satellite and the speed of the satellite towards the line of sight divided by the range of the satellite.

Writing a common equation composed of previously derived equations, the following form of equation is created (12):

$$\delta y = H \begin{bmatrix} \delta_{x'} \\ \delta_{y'} \\ \delta_{z'} \\ \delta_{b'} \end{bmatrix} + \begin{bmatrix} - & e^{(1)}/ & t \\ \vdots & \vdots & \vdots \\ - & e^{(K)}/ & t \end{bmatrix} \begin{bmatrix} \delta_x \\ \delta_y \\ \delta_z \end{bmatrix} + \varepsilon', \quad (12)$$

where:

$$\frac{\partial e^{(k)}}{\partial t} = \left(\frac{\partial(x^{(k)})}{\partial t} - e^{(k)} \cdot (e^{(k)} \cdot v^{(k)}) \right) \frac{1}{r^{(k)}}. \quad (13)$$

The presented below equation (13) is a linear equation regarding the position of the receiver, velocity and frequency shift in relation to the set of instantaneous measurements of the *Doppler* effect.

If the receiver is stationary, then the number of unknowns about δx , δy , δz and δb decreases. In this way, it is possible to solve the position of the navigation system receiver from the momentary Doppler measurements from four satellites.

4.2. Instrumentarium and experimental measurements

The measurements were carried out using a universal, single-frequency GPS + GLONASS L1 receiver, *Topcon* model GMS-2 equipped with an external antenna PG-A5. It is a 5-channel integrated satellite receiver with built-in digital compass, digital camera, connection in *Bluetooth* technology, universal serial port USB (*Universal Serial Bus*) and serial port.

In addition, the navigation system receiver has the ability to reduce multipath, so you can use it to perform static single-frequency, kinematic measurements. The differential global positioning system DGPS (*Differential Global Positioning System*) also has the ability to receive additional information and corrections from two systems, namely the US satellite assist system WAAS (*Wide Area Augmentation System*) and the European satellite-assisted system EGNOS (*European Geostationary Overlay Service*) [31], [32].

The image of the PG-A5 external antenna is shown in the figure below (Fig. 6).



Fig. 6. The PGA-5 antenna on the test point [34].

Control measurements were carried out in a continuous mode, where the measurement time at the point was 12 hours, while the observations were recorded in a 10-second interval. This resulted in 3508 3D position determinations. During measurement, the following variables were recorded: consecutive number of the measured point, coordinates (x, y, h) , mean coordinate errors calculated by the navigation system receiver at the time of measurement (Mx, My, Mh) , accidental error (Mp) , the value of the positional geometric coefficient of accuracy the PDOP (*Positional Dilution of Precision*) and the number of satellites observed [33], [34].

The results are summarized in tabular form and analyzed in detail in diagrams whose key purpose is to determine the availability and quality of EGNOS system corrections at a selected test point, illustrated in the above figure.

5 Results of tests carried out and analysis of obtained test results

5.1. Coordinate monitoring results on the test point using the EGNOS system service

Through the continuity of measurements of GPS system signals at the analyzed checkpoint, time series of high resolution coordinate solutions were generated, i.e. 10 [s]. They are presented in the figures below (Figures 7, 8 and 9). They contain local characteristics of various factors influencing the coordinate solution using the EGNOS system service.

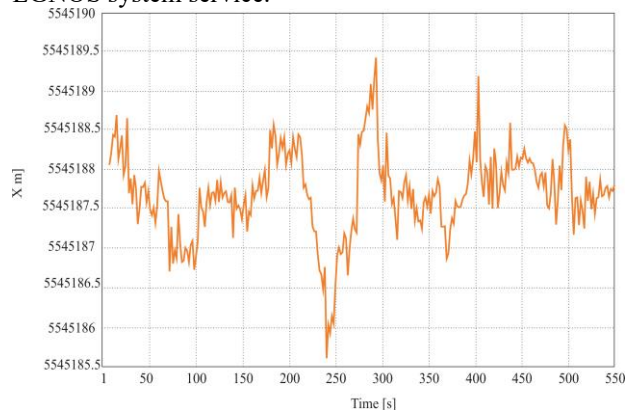


Fig. 7. Time series of the X coordinate obtained as a result of measurements at the test point.

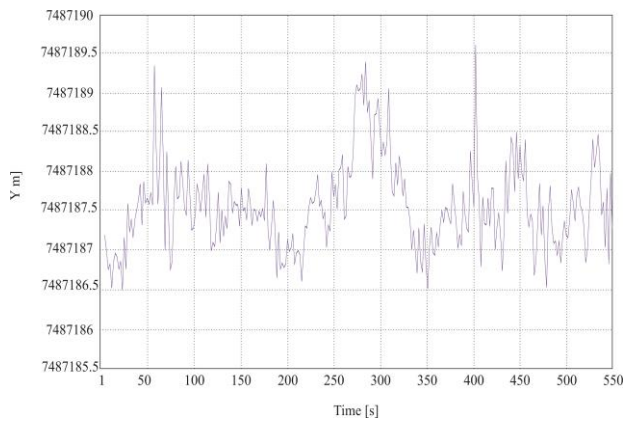


Fig. 8. The time series of the Y coordinate obtained as a result of measurements at the test point.

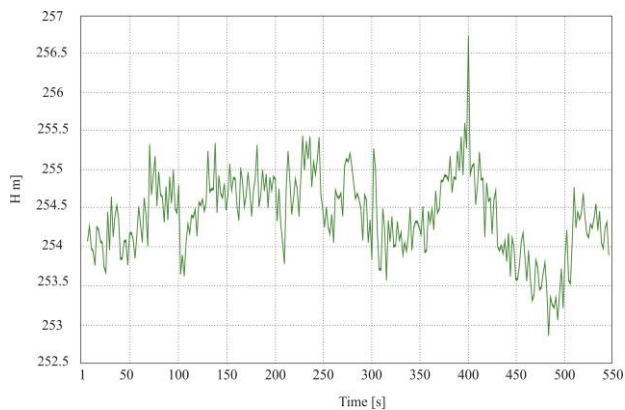


Fig. 9. The time series of the coordinate H obtained as a result of measurements at the test point.

Analysis of coordinate changes at the checkpoint as a function of time allows us to note some periodic changes in individual components and cases of increased fluctuation. In general, the scatter of measurement results for the X coordinate was 2.78 [m] with a standard deviation of 0.55 [m], for the Y coordinate 2.86 [m] with a standard deviation of 0.40 [m] and for the height coordinate H 5.09 [m] with a standard deviation of 1.04 [m].

5.2. Analysis of the obtained measurement results

The analysis of the obtained time series allows to draw a lot of conclusions on the accuracy, reliability and effectiveness of the obtained coordinate solutions in a given time interval from the EGNOS system service corrections used in the measurements.

For example, in the figure below (Fig. 10) the displacement measurement cycle (dx , dy , dh) is shown, the position determined from the "true" coordinates for individual variables (X , Y , H). Deviations for the X coordinate range from -0.13 to +2.65 [m], for the Y coordinate from -0.72 to +2.13 [m], and for the height H from -1.97 to +3.11 [m]. The next figure (Fig. 11) illustrates the comparison of medium errors (Mx , My , Mh), calculated by the instrument in the analyzed time series.

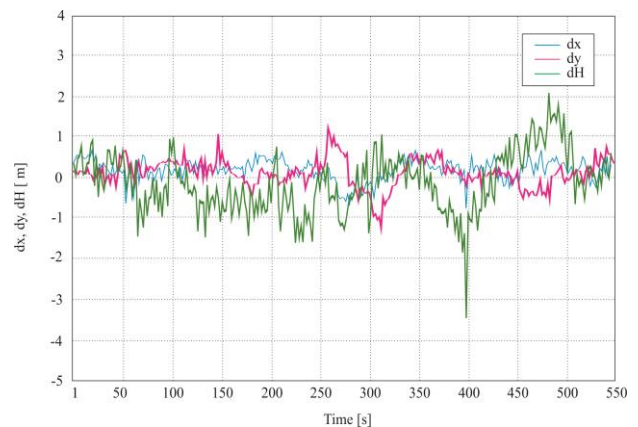


Fig. 10. Collective juxtaposition of differences of measured and catalog coordinates: dx , dy , dh .

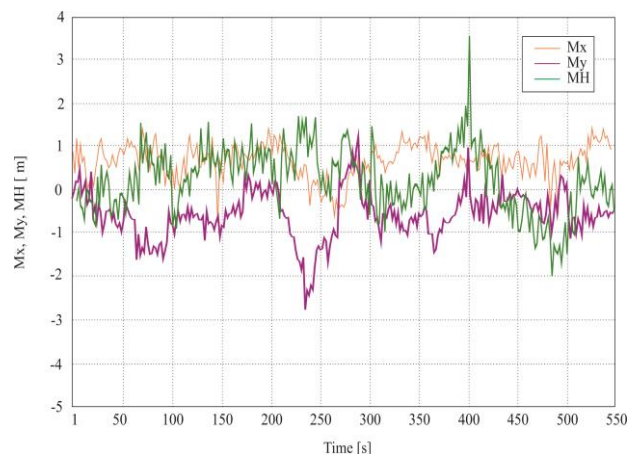


Fig. 11. Collective juxtaposition of medium errors of coordinates (Mx , My , Mh), determined and given by the instrument during the measurement.

Generated time series from coordinate solutions of points using the GMS-2 receiver assisted by correction of the EGNOS system service, enable qualitative and quantitative analysis of short-term changes in the determined coordinates based on the obtained GNSS system measurements [35], [36], [37], [38].

A detailed analysis of the obtained results allows to conclude that the GNS-2 receiver with EGNOS system correction increases the real positioning accuracy for the X coordinate to approximately 2.6 [m], for the Y coordinate to approximately 2.1 [m] and the height H to approximately 3.1 [m].

It should be noted, however, that average errors calculated by the receiver are characterized by low sensitivity to changes in the real coordinate value and its "true" error. Analysis of diagrams on the above figures (Fig. 10-11) showed that despite large deviations of coordinates measured, the medium error, especially for flat coordinates, does not change in a visible way.

The analysis also showed that with the use of the measuring set in question, the medium errors of the determined coordinates calculated by the instrument for the X coordinate are about 52 [%] lower, while for the coordinate Y by about 40 [%] smaller, in relation to the real measurement deviations.

6 Summary and Conclusions

The presented work presents the importance of further development of satellite navigation systems to obtain the most accurate measurement results. GNSS system services can provide precise positioning with global coverage as far as the receivers are able to connect with at least four satellites. This type of limitation is a major disadvantage of the GPS system, which leads to limited reliability [39], [40], [41].

A milestone in this process is undoubtedly the use of assistance data signals in the system with the A-GPS system receiver, where cellular positioning techniques have excellent reliability, especially in urban areas. Nevertheless, they can be improved by advanced mobile positioning, in particular by connecting to a wireless local area network.

Summing up, the results obtained on the basis of conducted tests can be seen that starting the operation of a conventional receiver is more than 0.5 [min], while for the receiver of the A-GPS support system, i.e. "cold start" can be 1 [s] or less. This is a very useful information for the aviation industry, because the shorter the time to determine the exact position of the aircraft, the safer, faster and more economically one can fly on them in specified conditions.

In addition, an important element of improving the positioning of the GPS system is its expansion by local satellite services, which were considered in this work (chapter 5). As demonstrated by the example of the EGNOS system, the corrections obtained through it are significant [42], [43].

The availability of the EGNOS system correction in the analyzed time series was approx. 81 [%]. It can be increased by the progress of implementation of RIMS (*Ranging and Integrity Monitoring Station*) ground stations, working for the needs of the service.

In addition, during the measurement a phenomenon was observed that the receiver of the navigation system used fewer satellites in relation to all available, because these satellites did not receive corrections from the EGNOS system. A necessary condition for a satellite to receive EGNOS system corrections is the need to keep track of at least 3 RIMS stations.

In the geographic areas of our country (Poland), this is mainly due to the small number of RIMS stations located east of the meridian of 21 degrees, because according to the EGNOS service area, defined in the 1990s, the eastern border of Poland is at the same time the eastern border of the EGNOS service system.

Positioning the GPS system with the use of EGNOS system correction allowed to obtain better results than positioning using the autonomous method. For example, the accuracy of the vertical component is particularly noticeable.

Therefore, to summarize the above analysis and the results of tests, supported by calculations and analysis of the obtained results, it can be concluded that satellite navigation systems work more accurately with the possibility of using assistance data and extensions obtained with the cooperation of several systems and

development of terrestrial infrastructure responsible for processing and further information transfer navigation.

In addition, it should be noted that the data presented in the paper are not final, because the whole positioning system is constantly developed for almost 50 years, which predicts hopes for a "more accurate" future.

References

1. M.W. Veal, S.E. Taylor, T.P. McDonald, D.K. Tackett, and M.R. Dunn, "Accuracy of Tracking Forest Machines with GPS," American Society of Agricultural Engineers, Volume 44(6), 2001
2. M. Thor, I. Eriksson, S. Mattson, "Real-time Monitoring of Thinning Performance Using Automatic Data Collection and GPS," Results, No. 2. Skogforsk, Uppsala, Sweden, 1997, pp. 1-4
3. L. Setlak, R. Kowalik, "Analysis, Mathematical Model and Selected Simulation Research of the GNSS Navigation Receiver Correlator," MATEC Web of Conferences, Volume 210, 2018
4. T. McDonald, "Time Study of Harvesting Equipment Using GPS-Derived Positional Data," Miscellaneous Publication, In Proceedings of the Forestry Engineering for Tomorrow, Edinburgh University, 1999, pp. 1-8
5. S.M. Prasanna Kumar, & S.K. Mahajan, "Economic Applications of GPS in Road Project in India," Procedia-Social and Behavioural Sciences, Volume 96, 2013, pp. 2800-2810
6. P. Yerma, & J.H. Bhatia, "Design and Development of GPS-GSM Based Tracking System with Google Map Based Monitoring," International Journal of Computer Science, Engineering and Applications (IJCSA), Volume 3(3), 2013, pp. 33-40
7. A.E. Rabbany, "Introduction to GPS: The Global Positioning System (2nd edition)," Artech House, 655 Canton Street, Norwood, MA 02062, 2006
8. P. Singal, & R.S. Chhillar, "A Review on GPS and its Applications in Computer Science," International Journal of Computer Science and Mobile Computing, Volume 3(5), 2014, pp. 1295-1302
9. S. Gobi, "Introduction to GPS: Principles and Applications," Tata McGraw-Hill Publishing Company Limited, New Delhi
10. S. Hwang & D. Yu, "GPS Localization Improvement of Smart Phones Built in Sensors," International Journal of Smartphone, Volume 6(3), 2012
11. Paul Zandbergen, "Accuracy of iPhone Locations: A Comparison of Assisted GPS, WiFi and Cellular Positioning," Blackwell Publishing Ltd, Transactions in GIS, Volume 13(s1), 2009, pp. 5-26
12. M.J. Duncan, H. M. Blandall & W. K. Mummery, "Applying GPS to Enhance Understanding of Transport-related Physical Activity," Journal of Science and Medicine in Sport, Volume 10(10), 2008

13. L. Setlak, R. Kowalik, "MEMS Electromechanical Microsystem as a Support System for the Position Determining Process with the Use of the Inertial Navigation System INS and Kalman Filter," *WSEAS Transactions on Applied and Theoretical Mechanics*, Volume 14, 2019
14. C. Hentry, K. Saravanan's and Kulathuran, "Application of GPS in Fisheries and Marine Studies," *International journal of Advance Research in Computer Science*, Volume 2(6), 2011
15. M. PirBavaghar, H. Sobhani. J. Fegghi, A.A. Darvishsefat, M.R. Marvi-Mohajer, *Journal of Forest and Poplar Research*, Volume 32(4), 2007, pp. 374-385
16. N. O. Tippenhauer, K. B. Rasmussen, C. Pöpper, and S. Capkun, "Attacks on Public WLAN Based Positioning Systems," In *Proceedings of the ACM/Usenix International Conference on Mobile Systems, Applications and Services (MobiSys '09)*, Kraków, Poland, 2009
17. F. van Diggelen, *A-GPS "Assisted GPS, GNSS and SBAS"*, Artech House, London, 2009
18. Vancouver and Whistler, *British Columbia Skyhook Wireless "Wi-Fi Positioning System: Accuracy, Availability and Time to Fix Performance"*, Boston, MA, Skyhook Wireless Technical White Paper, 2008
19. M. Edwards C., and B. McCarthy, "A Study of LBS Accuracy in the UK and a Novel Approach to Inferring the Positioning Technology Employed," *Computer Communications*, Volume 31, 2008, pp. 1148-1159
20. Navizon "Bringing Wi-Fi and Cellular Positioning to Mobile Devices and to the Web," New York, Mexens Technology, Inc., Navizon Technical Paper, 2007
21. K. Kaemarungsi and P. Krishnamurthy, "Modeling of Indoor Positioning Systems Based on Location Fingerprinting," In *Proceedings of IEEE Infocom*, Hong Kong, 2004, pp. 1012-1022
22. F. Gustafsson and F. Gunnarsson, "Mobile Positioning Using Wireless Networks: Possibilities and Fundamental Limitations Based on Available Wireless Network Measurements," *IEEE Signal Processing Magazine*, Volume 22(4), 2005, pp. 41-53
23. Mike Y. Chen, Timothy Sohn, Dmitri Chmelev, Dirk Haehnell, Jeffrey Hightower1, Jeff Hughes, Anthony LaMarca, Fred Potter, Ian Smith, Alex Varshavsky, "Practical Metropolitan-Scale Positioning for GSM Phones," In *Proceedings of the International Conference on Ubiquitous Computing*, Newport Beach, California, UbiComp 2006, pp. 225-242
24. L. Setlak, R. Kowalik, "Mathematical Modeling and Simulation of Selected Components On-board Autonomous Power Supply System (ASE), in Accordance with the Concept of a More Electric Aircraft (MEA)," *IEEE Xplore*, 2017
25. A. Kushki, K. N. Plataniotis, and A. N. Venetsanopoulos, "Kernel Based Positioning in Wireless Local Area Networks," *IEEE Transaction on Mobile Computing*, Volume 6, 2007, pp. 689-705
26. T. S. Lin and P. C. Lin, "Performance Comparison of Indoor Positioning Techniques Based on Fingerprinting," In *Proceedings of the Sixth IEEE International Symposium on a World of Wireless Mobile and Multimedia Networks*, Taormina, Italy, 2005, pp. 382-387
27. T. Manodham, L. Loyola, T. Miki, "A Novel Wireless Positioning System for Seamless," *Internet Connectivity Based on the WLAN Infrastructure*, *Wireless Personal Communication*, Volume 44(3), 2008, pp. 295-309
28. A. Bensky, "Wireless Positioning Technologies and Applications," Artech House Inc., Boston, MA 02062, 2008
29. W. Branford, James Parkinson & J. Spilker, "Global Positioning System: Theory and Applications," *American Institute of Aeronautics*, Lincoln, NE, U.S.A, Volume 1, 1996
30. Per K. Enge, "Global Positioning System: Signals, Measurement and Performance," *International Journal of Wireless Information Networks*, Volume 1(2), 1994, pp. 83-105
31. S. Ekahau Gezici "A Survey on Wireless Positioning Estimation," *Wireless Personal Communication*, Volume 44, 2008, pp. 263-282
32. A. J. Weiss, "On the Accuracy of a Cellular Location System Based on RSS Measurements," *IEEE Transactions on Vehicular Technology*, Volume 52, 2003, 1508-1518
33. A. Schwaighofer, M. Grigoras, V. Tresp, and C. Hoffmann, "GPPS: A Gaussian Process Positioning System for Cellular Networks," In *Proceedings of Neural Information Processing Systems*, 2003
34. J. Yim. "Introducing a Decision Three-based Indoor Positioning Technique," *Expert Systems with Applications*, Volume 34, 2008, pp. 1296-1302
35. K. W. Kolodziej and J. Hjelm, "Local Positioning Systems: LBS Applications and Services," BocaRaton, FL, Taylor and Francis, 2006
36. S.A. Golden, and S.S. Bateman, "Sensor Measurements of Wi-Fi Location with Emphasis on Time-of-Arrival Ranging," *IEEE Transactions on Mobile Computing*, Volume 6(10), 2007, pp. 1185-1198
37. L. Setlak, R. Kowalik, "Examination of Multi-Pulse Rectifiers of PES Systems Used on Airplanes Compliant with the Concept of Electrified Aircraft," *Applied Sciences (Switzerland)*, Tom 9, Wydanie 8, 2019/1
38. Paramvir Bahl and Venkata N. Padmanabhan, "Enhancements to the RADAR User Location and Tracking System," Redmond, WA, Microsoft

Research Technical Report No. MSR-TR-2000-12,
February 2000

39. P. Misra, & P. Enge, "Global Positioning System: Signals, Measurement and Performance," Ganga-Jamuna Press, P.O. Box 633, Lincoln, Massachusetts-01773, 2010
40. S. Juurakko and W. Backman, "Database Correlation Method with Error Corrections for Emergency Location," *Wireless Personal Communications*, Volume 30(2-4), 2004, pp. 183-194
41. W. Mironiuk, "Influence of Flooding Compartment on the Ship's Safety," *WSEAS Transactions on Applied and Theoretical Mechanics*, Volume 12, 2017, pp. 188-194
42. M. Wallbaum, "A Priori Error Estimates for Wireless Local Area Network Positioning Systems," *Pervasive and Mobile Computing*, Volume 3, 2007, pp. 560-580
43. D.B. Lin and R.T. Juang, "Mobile Location Estimation Based on Differences of Signal Attenuations for GSM Systems," *IEEE Transactions on Vehicular Technology*, Volume 54, 2005, pp. 1447-1454